Oil and Air Dispersion in a Simulated Fermentation Broth as a Function of Mycelial Morphology

Savidra Lucatero,[†] Claudia Patricia Larralde-Corona,[‡] Gabriel Corkidi,[§] and Enrique Galindo*[,†]

Instituto de Biotecnología and Centro de Ciencias Aplicadas y Desarrollo Tecnológico, Universidad Nacional Autónoma de México, Apdo Post. 510-3, Cuernavaca, Morelos 62250, Mexico, and Centro de Biotecnología Genómica-IPN, Apdo. Postal 152, Reynosa, Tamaulipas 88710, Mexico

The culture conditions of a multiphase fermentation involving morphologically complex mycelia were simulated in order to investigate the influence of mycelial morphology (*Trichoderma harzianum*) on castor oil and air dispersion. Measurements of oil drops and air bubbles were obtained using an image analysis system coupled to a mixing tank. Complex interactions of the phases involved could be clearly observed. The Sauter diameter and the size distributions of drops and bubbles were affected by the morphological type of biomass (pellets or dispersed mycelia) added to the system. Larger oil drop sizes were obtained with dispersed mycelia than with pellets, as a result of the high apparent viscosity of the broth, which caused a drop in the power drawn, reducing oil drop break-up. Unexpectedly, bubble sizes observed with dispersed mycelia were smaller than with pellets, a phenomenon which can be explained by the segregation occurring at high biomass concentrations with the dispersed mycelia. Very complex oil drops were produced, containing air bubbles and a high number of structures likely consisting of small water droplets. Bubble location was influenced by biomass morphology. The percentage (in volume) of oil-trapped bubbles increased (from 32 to 80%) as dispersed mycelia concentration increased. A practically constant (32%) percentage of oil-trapped bubbles was observed with pelleted morphology at all biomass concentrations. The results evidenced the high complexity of phases interactions and the importance of mycelial morphology in such processes.

Introduction

Filamentous fungi are commercially important microorganisms for the production of many metabolites (*1*), including pharmaceuticals, most of antibiotics, enzymes, organic acids, proteins, and some aroma compounds (*2*, *3*).

An important operation in fermentation processes is to provide a sufficient supply of substrates to the microorganism. Some substrates, including air and oils, require mechanical dispersion into the aqueous medium. In such cases, the interfacial area for mass transport significantly determines the rate of metabolic reactions, biomass growth, and metabolites yields. In processes using oils as a sole carbon source, high substrate dispersion in the liquid phase is required in order to promote high lipase biosynthesis rates for subsequent substrate degradation. A difficulty found when dispersing oils is their low availability (*4*) due to the hydrophobic nature of oils and their tendency to reduce interfacial area in aqueous media. High substrate accessibility to the organism is achieved when the area/volume ratio of oil droplets is increased (*5*). Therefore, the measurements of drop and air bubble sizes are highly relevant. Mean size and size distribution of drops depend on hydrodynamic conditions in the system and on physical properties of liquids (*6*). Drop break-up occurs when shear stresses of the continuous phase, responsible of drop deformation, exceeds the stabilizing interfacial tension forces and internal viscous stresses which oppose deformation (*7*).

In fermentation processes involving filamentous microorganisms, oil and gas dispersion might become further limited as a consequence of mycelial growth, especially when the microorganism grows in the dispersed form (freely dispersed mycelia and clumps). The presence of mycelial particles considerably increases the viscosity and the non-Newtonian behavior of suspensions, leading to highly coalescent systems, where interfacial area for mass transport is reduced (*8*). Furthermore, the formation of stagnant zones away from the impeller region might affect phase dispersion, enhancing coalescence or hindering the transport of air bubbles and oil drops throughout the vessel. In these zones, bulk mixing and substrate dispersion are rather poor, limiting nutrient transport to the microorganism (*9*). On the other hand, pellet suspensions have considerably different rheological characteristics, being low-viscosity systems, which is convenient for high mass transport (*10, 11*).

Some authors have mentioned that interfacial area for mass transfer is affected in fermentation broths containing dispersed mycelia or pellets (*12*−*14*). However, no quantitative and/or systematic studies in this specific

* Corresponding author. Fax: +52 777-317-2388. E-mail: galindo@ibt.unam.mx.

[†] Instituto de Biotecnología, Universidad Nacional Autónoma de México.

[‡] Centro de Biotecnología Genómica-IPN.

[§] Centro de Ciencias Aplicadas y Desarrollo Tecnológico, Universidad Nacional Autónoma de México.

10.1021/bp020118e CCC: $25.00
Published on Web 02/06/2003

subject have been published. There are studies focusing on characteristics of flow patterns and gas dispersion properties for viscous and non-Newtonian systems, using noncoloring viscosifying agents such as carboxymethyl cellulose (CMC) or xanthan gum (*15*−*17*). Nonetheless, a suspension of mycelial particles considerably differs from these homogeneous systems (*18*). Furthermore, when considering the applicability of a correlation to estimate the average drop diameter, very few models have been proposed for viscous, non-Newtonian systems. Turbulence damping occurring when the continuous phase is viscous does not justify the applicability of the Kolmogoroff theory of isotropic turbulence in predicting the minimum drop size in such systems (*19*). Shimizu et al. (*17*) have proposed a model to estimate drop size in non-Newtonian aqueous phases. By maintaining a low volume fraction of the dispersed phase, drop sizes were assumed to depend mainly on breakage and to be independent of coalescence; however, some coalescence is expected to occur in viscous non-Newtonian liquids (*17*).

Previous studies addressing immiscible substrate dispersions on fermentation systems include that of Galindo et al. (*20*), who investigated the behavior of oil drop and air bubble sizes in the presence of mycelial biomass. As biomass concentration was increased, decreases in both drop and bubble mean diameters were found. More recently, Larralde et al. (*21*) published data concerning air dispersion in viscous simulated broths, dealing with the location of air bubbles. These authors reported an increasing volume of oil-trapped bubbles as a function of biomass concentration. However, none of the previous works took into account the influence of mycelial morphology on oil and gas dispersion.

The present work focused on establishing the effect of mycelial morphology (i.e. pellets and dispersed mycelia, the latter including freely dispersed and long loose clumps) on oil and air dispersions in a model fermentation system. This system simulates a multiphase fermentation system, in particular that for the production of the γ-decalactone (*2*) by *Trichoderma harzianum* (*T. harzianum*), which includes an aqueous phase (salt-rich media), air, mycelia (solid phase), and a water immiscible oil phase as the sole carbon source.

Materials and Methods

Strain and Culture Conditions. *Trichoderma harzianum* IMI 206040 was used, and conventional procedures were used to maintain the strain and to develop seed cultures. Dispersed mycelia production was carried out in a 14 L bioreactor (New Brunswick Scientific, New Brunswick, NJ), with 10 L of working volume, equipped with four equally spaced baffles ($d/T = 0.1$) and three six-blade Rushton turbines ($D/T = 1/3$), operating at 3.33 s^{-1}. Aeration was achieved through a ring sparger with five orifices of 1 mm. Initially, aeration rate was adjusted to 0.4 vvm and increased to 1 vvm after 36 h until the end of the culture (72 h). If necessary, a few drops of a silicon-based antifoaming agent were added. Pelleted morphology was produced in 500 mL shake flasks with 100 mL of culture medium. The shaker (New Brunswick Scientific) was operated at 3.33 s^{-1}, and the culture time was 108 h. The temperature of culture medium was maintained at 29 °C. The spore inoculum concentration was 10^4 and 10^3 spores/mL, for pellets and dispersed mycelia production, respectively. Prior to sterilization, the initial pH of the culture media was adjusted to 3.2 (bioreactor) and 5.6 (flasks) with concentrated H_3PO_4 to produce dispersed mycelia and pellets, respectively. The pH was not further controlled.

Morphological Measurements. Morphological measurements of mycelial particles and the percentage of aggregates in the sample were determined using an image analysis system consisting of a CCD camera (Nikon Color, KP-D50) coupled to a microscope (Nikon Optiphot-2) or a CCD camera (Nikon KP-160) mounted to a stereomicroscope (Olympus SZ40) and a PC with the image analysis software (Image Pro Plus 4.1, Media Cybernetics, Silver Spring, MD) installed. At least 300 mycelial particles were analyzed for each sample. Morphological parameters measured were diameter, circularity, and compactness. Circularity describes the deviation of mycelial particles from a true circle, and compactness gives an estimation of hyphal entanglement density (*22*). Both parameters were calculated as described by Thomas (*22*).

Biomass Concentration. Biomass concentration was evaluated by dry weight. Samples of 10−50 mL were filtered through a membrane (Whatmann, 0.45 μm pore size) and rinsed with twice their volume of distilled water. Cakes obtained were left for 24 h in an oven at 95 °C, then placed overnight in a desiccator, and weighted afterward.

Rheological Measurements. Rheological measurements were carried out at 29 °C using a Rheomat 120 rheometer (Contraves, Zurich, Switzerland) fitted with a helicoidal ribbon impeller at shear rates ranging from 0.03 to 330 s^{-1}.

Stirred Tank. To simulate the culture conditions of an actual fermentation and to carry out castor oil and air dispersion studies, a glass cylindrical flat-bottomed stirring tank was employed. The tank had an internal diameter (T) of 0.21 m with four equally spaced baffles (0.021 m) and one six-blade Rushton turbine ($D/T = 0.5$). The cylindrical tank was surrounded by a square plexiglass jacket, filled with circulating water to maintain the temperature at 29 ± 0.1 °C and also working as a correcting lense to reduce light distortion. The working volume was 6.7 L, with a liquid depth equal to the internal vessel diameter. The shaft, impeller, baffles, and air supply tube were constructed with stainless steel. Filtered air was introduced to the mixing tank through a sintered sparger with an average pore size of 20 μm (Waters Chromatography, Bedford, MA) located below the impeller.

The mixing tank used in this study was coupled to an accurate air bearing dynamometer (*23*) for power drawn measurements. The torque exerted by the stirrer to the fluid was assessed by measuring the force acting on an electronic balance. The arithmetic mean of 20 torque readings was taken to calculate the power applied. The error estimated was less than 1%.

Image Analysis Equipment. Images of the dispersion were obtained in situ by using a developed purpose-made video-microscope-computer system described elsewhere (*24*). From 100 to 300 images were taken to measure at least 500 drops, the number of objects that preliminary experiments indicate necessary to ensure an error lower than 5% in drop size measurements. Reproducibility of experiments was high; for example, two independent runs (without biomass) were carried out under identical operating conditions (agitation speed, aeration rate, volume fraction of the dispersed phase), and the Sauter diameter values were 1222 and 1214 μm; the difference between two runs was around 10 μm, which means a standard deviation on drop size measurements of less than 2%.

Having the diameter data, the mean Sauter diameter and the number probability density distributions were

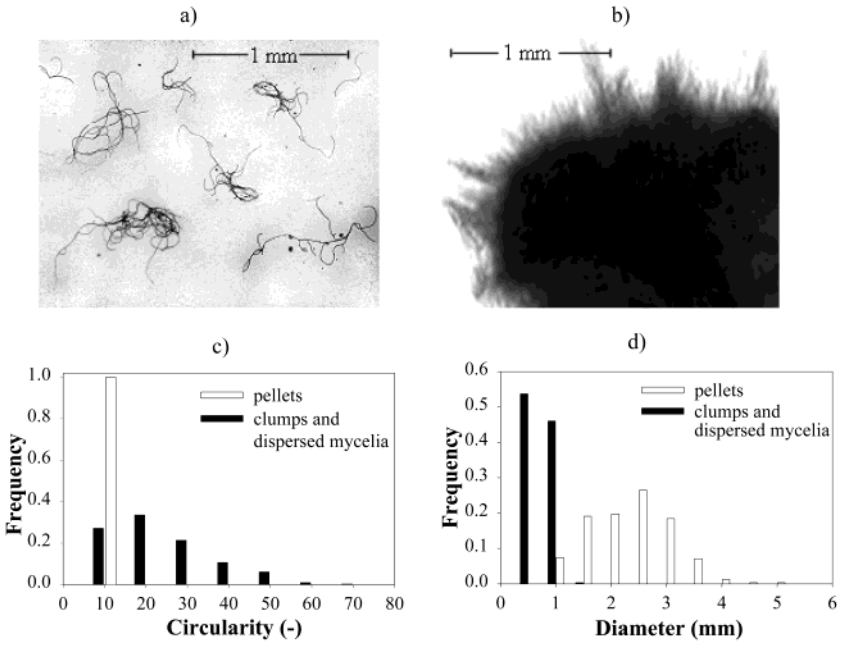

Figure 1. Typical images of dispersed mycelia (a) and pellets (b). Frequency distributions of roughness (c) and diameter (d) for both types of biomass.

determined, which were useful for illustrating the effect considered in the present work. Additionally, the average number of objects per frame proved useful in illustrating the relative amount of objects in the image capture zone. This parameter was calculated by counting all the bubbles in a series of images and then dividing by the number of images. Also, the average volume of bubbles per frame was used as a quantitative estimation of the amount of gas dispersed in the image capture region. For this, the total volume of a population of bubbles was divided by the number of images containing those bubbles.

Dispersion Experiments Procedure. The continuous phase consisted of 6.3 L of aqueous media (simulating a fermentation broth) with the following composition (g/L): $(NH_4)_2SO_4$ (5), KH_2PO_4 (7), $NaHPO_4$ (2), $MgSO_4$ (1.5), $CaCl_2 \cdot 6H_2O$ (0.067), $ZnSO_4 \cdot 7H_2O$ (0.0001), $FeCl_3 \cdot 6H_2O$ (0.008). The dispersed phase was food-grade castor oil (Cosmopolita, Mexico), which is a combination of fatty acids (mainly ricinoleic acid) having a viscosity of 560 mPa s at 26 °C.

The biomass harvested (from bioreactor or flasks) was collected and rinsed with abundantly distilled water to eliminate the exhaust media. In the case of pellets, biomass was simultaneously sieved through a stainless steel sieve (with 2.5 mm grid) to eliminate any fraction of dispersed mycelia. The concentrated (aproximately 25−30 g/L) rinsed biomass was used for dispersion experiments immediately after being harvested. During the experiment, the biomass was maintained at 4 °C and a volume of this biomass was taken and added every 30 min to the mixing tank where an experiment was being carried out. Special care was taken in the washing and cleaning of the glass tank and stainless steel material. The tank was first filled with the aqueous phase and then with the oil. The dispersed (oil) phase was 5% (v/v). Later, agitation speed and aeration rate were adjusted to 3.33 s^{-1} and 1.675 mL/min (0.25 vvm), respectively. Such agitation speed corresponded to a power drawn of 0.26 $\pm$ 0.01 and 0.18 $\pm$ 0.01 W/L for the ungassed and gassed conditions, respectively. A stabilizing time of 2 h before taking the first set of images (for the control run, without biomass) and 30 min for subsequent captures was previously estimated long enough for a steady state to be reached.

Table 1. Morphological Charactistics of the Biomass Used and the Rheological Properties of Their Suspensions

parameter	dispersed mycelia and clumps			pellets		
diameter (mm)	0.04−1			0.5−5		
circularity	0.015−0.3			0.05−1		
compactness (%)	0.2−1			0.9−1		
biomass (g/L)	0.5	1.3	3.2	0.1	1.3	3.2
consistency index (K)	0.04	0.35	1.6	0.01	0.1	0.14
flow index (*n*)	0.78	0.40	0.39	0.90	0.72	0.63

Results and Discussion

Morphological Characteristics of Pellets and Dispersed Mycelia. Figure 1 shows typical images of both the pelleted and the dispersed morphologies of *Trichoderma harzianum* produced. Mean diameter, circularity, and compactness of mycelial particles, as well as the percentage of mycelial clumps in the sample of dispersed mycelia, were determined, as they significantly affect the rheological properties of mycelial suspensions (*13, 25, 26*). For comparative purposes, circularity and diameter frequency distributions for both morphological types of biomass used are also shown in Figure 1. Pellets were compact and smooth and showed larger mean diameters, as well as higher compactness than dispersed mycelia. Circularity was smaller for pellets than for dispersed mycelia (Table 1). Under the conditions of dispersed morphology production, more than 70% of the hyphae were as long loose clumps, which could explain the increase in the consistency index and the decrease in the flow index of the power law model, with biomass concentration (Table 1). Using the pelleted morphology, no significant changes in the power law model parameters with biomass concentration were observed (Table 1).

Influence of Mycelial Morphology on Oil Dispersion. Figure 2 shows typical images of oil and air

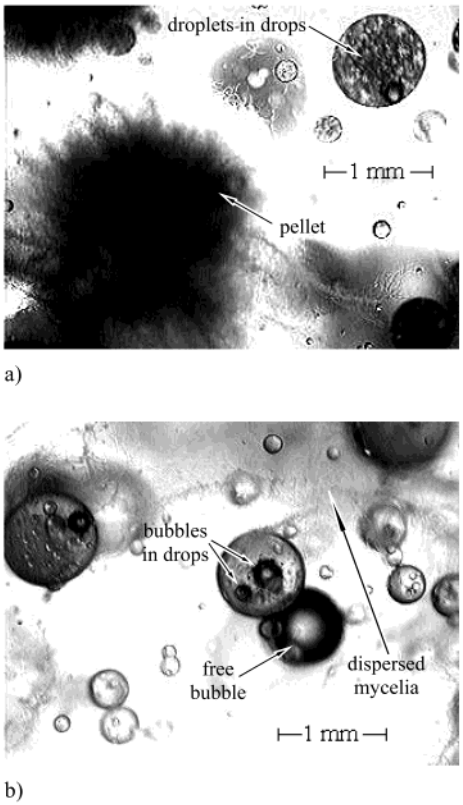

Figure 2. Typical images of the oil and air dispersion with pelleted (a) and dispersed (b) morphologies of the biomass.

dispersion with the pelleted and the dispersed morphologies. Figure 3 shows how the Sauter diameter of oil drops was affected by mycelial morphology and concentration. Dispersed mycelia caused a slight decrease in the Sauter diameter of oil drops at biomass concentrations lower than 1.7 g/L, and smaller oil drop sizes were generated with dispersed mycelia than with pellets. However, at higher concentrations of dispersed mycelia a further increase in oil drop sizes was observed, and larger oil drop sizes were obtained with dispersed mycelia than with pellets (Figure 3). In the system with pellets, the Sauter diameter of oil drops was practically unaffected over the whole range of biomass concentrations studied.

It is likely that the slight decrease in the Sauter diameter of oil drops at biomass concentrations less than 1.7 g/L was a result of the attachment of mycelial particles to bubbles and to oil drops. This could hinder the immersion of bubbles in oil drops (see next section) or drop coalescence; consequently, a slight decrease in oil drop sizes was observed when dispersed mycelia were present (Figure 3). The solid particle adhesion to bubbles has been reported to occur when particles are hydrophobic (*27*). In the case of a filamentous fungus, it is well-known the hydrophobic properties of their cell membrane (*28*). Mycelial particle attachment to bubbles and drops was further confirmed in various snap images.

At biomass concentrations higher than 1.7 g/L, drop coalescence seems to be favored rather than inhibited by mycelial particles, and a further increase in the Sauter diameter of oil drops was observed (Figure 3), which can be explained by changes in the rheological properties of the suspensions. With increasing biomass concentration, broth viscosity considerably increases and an enhanced coalescence is expected to occur; consequently, larger oil drop sizes were observed. In addition, in the system with

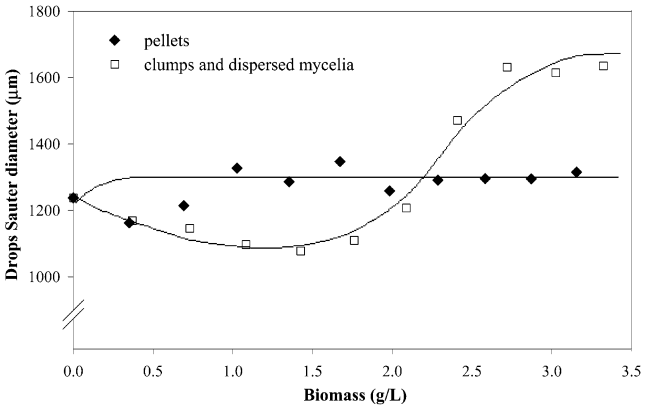

Figure 3. Influence of mycelial morphology and concentration on Sauter diameter of oil drops.

dispersed mycelia, a drop of up to 50% in power drawn (data not shown) with increasing biomass concentration (from 1.7 to 3.4 g/L) is consistent with larger oil drop sizes observed, since drop sizes are expected to increase with decreasing energy dissipation rate (*29*). Pellets did not significantly affected the Sauter diameter of oil drops (Figure 3), probably as a consequence that broth viscosity remained unchanged, since neither consistency nor flow indexes were significantly affected with biomass concentration (see Table 1).

Influence of Mycelial Morphology on Gas Dispersion. The influence of mycelial morphology and concentration on the Sauter diameter of air bubbles is shown in Figure 4. Smaller bubble sizes were generated with dispersed mycelia than with pellets. The presence of dispersed mycelia in the mixing tank decreased the Sauter diameter of bubbles when the biomass concentrations were higher than 1.5 g/L. For example, dispersed mycelia at 3.1 g/L caused a reduction of approximately 43% in the Sauter diameter of bubbles compared to the system without biomass. In the system with pellets, the Sauter diameter of bubbles remained practically constant over the range of biomass concentrations analyzed.

On the snap images (i.e. Figure 2), it was possible to distinguish easily air bubbles inside the oil drops, since air bubbles are shinning black and the drops are lighter with a dark perimeter. Bubble immersion in oil drops was first observed by Galindo et al. (*20*) in a system similar to that used in the present study. The bubble inclusion mechanism in oil drops probably occurs by drop deformation spreading around the bubble (*30*).

The size of both the oil-trapped bubbles and the free in the aqueous phase bubbles is shown as a function of mycelial morphology and concentration (Figure 5). In all cases studied, oil-trapped bubbles were smaller than free bubbles. With the pelleted morphology, the Sauter diameter of free bubbles was around 1.5-fold larger than for oil-trapped bubbles in the whole biomass range analyzed. With dispersed mycelia, this difference was progressively lower with increasing biomass concentration. The smaller sizes of oil-trapped bubbles could probably be due to the fact that, once inside the oil drop, a bubble is practically unable to coalesce (*21*). The Sauter diameter of both, the free and the oil-trapped bubbles (Figure 5) changed with biomass concentration and morphology, basically in the same way as total bubbles (oil trapped plus free ones, Figure 4). The size of both oil-trapped and free bubbles was smaller with dispersed mycelia than with pellets. Also, an increase in the dispersed mycelia concentration caused a decrease in the Sauter diameter of free and oil-trapped bubbles; however,

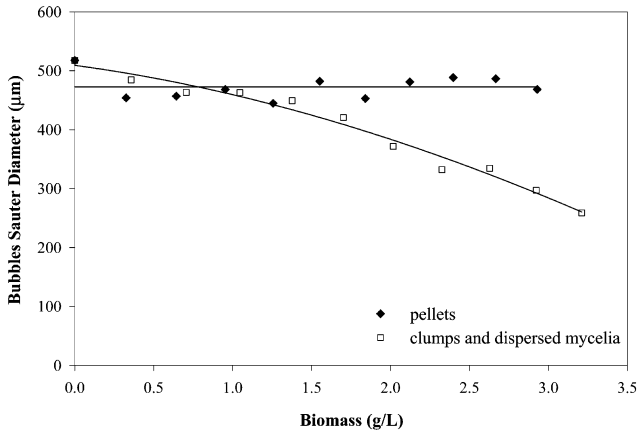

Figure 4. Influence of mycelial morphology and concentration on the Sauter diameter of air bubbles.

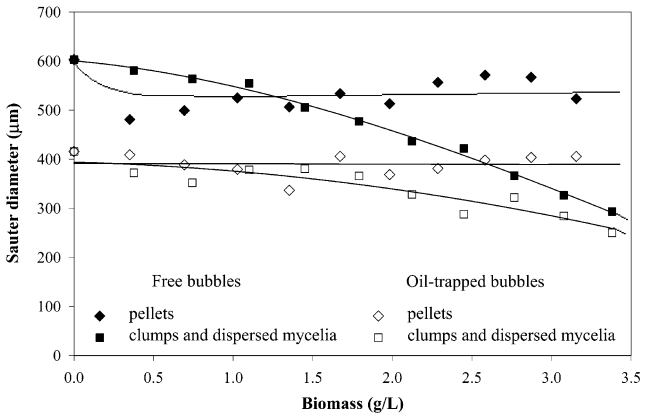

Figure 5. Effect of mycelial morphology and concentration on the Sauter diameter of free and oil-trapped air bubbles.

this decrease was more pronounced for free bubbles than for oil-trapped bubbles. Again, neither the Sauter diameter of oil-trapped nor that of free bubbles were significantly affected with biomass concentration in the system with pellets.

Figure 6 illustrates how the size distributions of free and oil-trapped bubbles changed with biomass concentration and morphology. With the pelleted morphology, the size distributions of free bubbles were wide, bell-shaped, and long-tailed (Figure 6a), while for oil-trapped bubbles they were less symmetric and narrower (Figure 6c) than those for free bubbles. Nevertheless, in both cases, the size distributions practically overlapped for different biomass concentrations (Figure 6a,c). This overlapping suggests that the presence of pellets seems to have no effect on size distributions of either free or oil-trapped bubbles and agree with no significant changes observed in the Sauter diameter of free and oil-trapped bubbles with increasing biomass concentration (Figure 4).

With dispersed mycelia, the size distributions of free and oil-trapped bubbles were wide and long-tailed, at low biomass concentrations. At higher biomass concentrations, the distributions became taller and narrower and their peak and tail shifted toward smaller diameters (Figure 6b,d). This shift to smaller diameters was less pronounced for oil-trapped bubbles and was consistent with a gradual decrease in the Sauter diameter of free and oil-trapped bubbles as dispersed mycelia concentration increased (Figure 4).

Contrary to oil drop size observations (Figure 3), bubble sizes decreased as the dispersed mycelia concentration increased (Figure 4). The smaller sizes and a narrowing in the size distributions of air bubbles observed in the high-viscosity suspension with dispersed mycelia contradicts the expected larger bubble sizes and a broadening in size distributions (as a consequence of enhanced coalescence). These results could be explained as follows: an increase in biomass concentration arises in highly viscous and shear thinning behavior of the aqueous phase, which could induce changes in the spatial distribution of air bubbles in the mixing tank, and, consequently, the data obtained corresponding to a specific location inside the tank might not be the same throughout the vessel. This was evidenced by the fact that a well-mixed zone surrounded by stagnant regions near the mixing tank wall were observed, a phenomenon also seen in the actual fermentation (*31*). The high-viscosity and non-Newtonian character of the broth containing dispersed mycelia could hinder the transport of big bubbles (formed by coalescence) toward the tank walls. It is likely that at highest biomass concentrations, the air stream is limited to the central region of the mixing tank. Our observations strongly suggest that big bubbles tend to rise by the center of the mixing tank, causing a channeling, as dispersed mycelia concentration increases. This was confirmed by visual observations of big bubbles breaking up at the liquid surface around the shaft, and not close to the mixing tank wall. Hence, only small bubbles followed the impeller radial flow patterns and were able to reach the wall so they could be measured, since the image capture point is located close to the vessel wall. These observations explain the sharp decrease in the Sauter diameter and a narrowing in the size distributions of air bubbles with increasing concentrations of dispersed mycelia (Figures 5 and 6b, respectively). As biomass concentration increased, a lower number of bubbles (oil-trapped or free) were observed in the snap images. At the highest biomass concentrations studied, only few small bubbles (free or oil-trapped) were seen and the bigger ones were practically absent in the images. These observations suggested a lower amount of gas dispersed in the wall region. Figure 7a and b respectively show a sharp decrease in the number and volume of free bubbles per frame with dispersed mycelia concentration, which further confirms a gradually lower amount of gas dispersed as free bubbles with increasing biomass concentration. A reduction of approximately 70% in both the number and volume of free bubbles per frame was determined between the minimum and maximum biomass concentrations analyzed (see Figure 7a,b). On the other hand, pellets caused only a slight decrease in the number and volume of free bubbles per frame (see Figure 7a,b, respectively), suggesting that this morphology did not affect the distribution of free bubbles throughout the vessel, at least at the biomass concentrations studied here. Our data suggest that the location of the image capture point has to be taken into account before concluding about the degree of dispersion inside a tank, as, even in a small tank as the one used in this work (at a relatively low power drawn), the size distributions could not be the same at different locations throughout the vessel. Consequently, in the case of high viscosity fluids (i.e. containing dispersed mycelia), the dispersion data obtained are only valid for regions adjacent to the tank wall. Because of the opacity of mycelial suspensions, measurements at neither greater depth through the wall (closer to the impeller) nor higher biomass concentrations were possible to analyze.

With dispersed mycelia, the Sauter diameter (Figure 5) of oil-trapped bubbles was also smaller as biomass

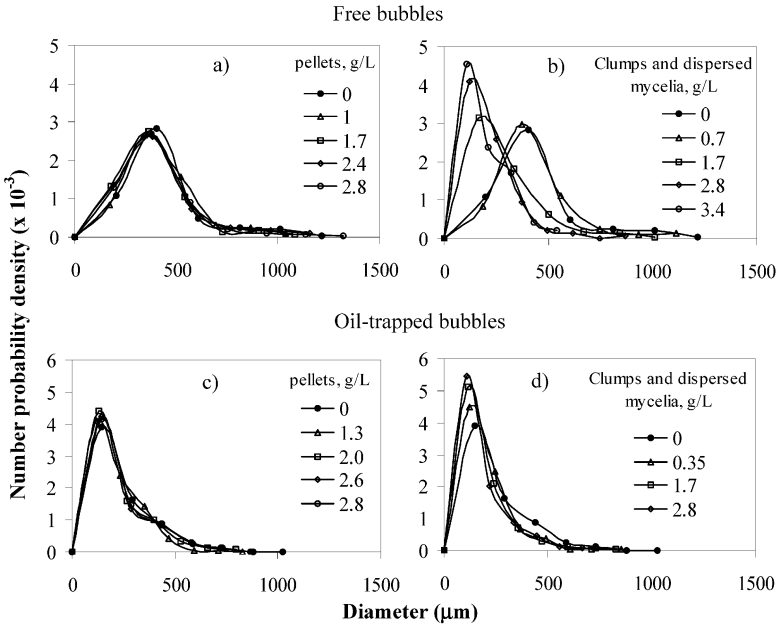

Figure 6. Number probability distributions of free (a, b) and oil-trapped (c, d) air bubbles, as a function of mycelial morphology and concentration.

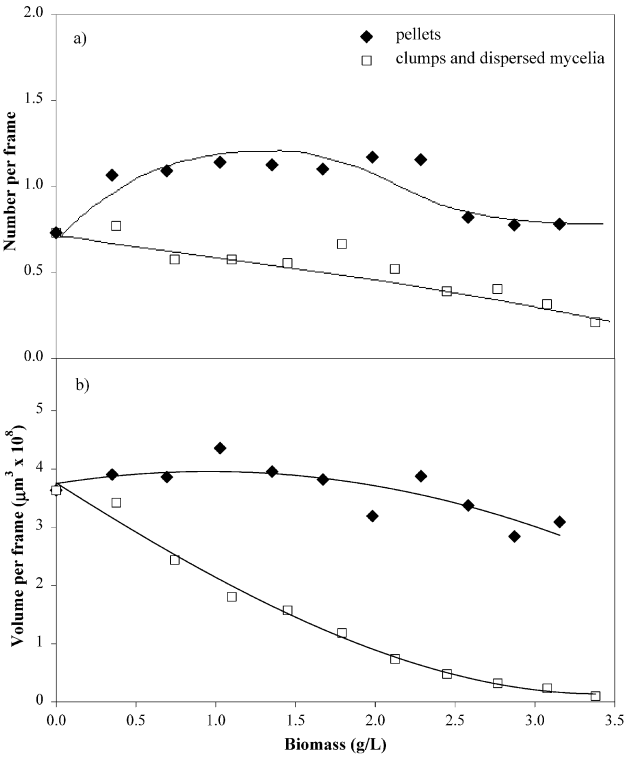

Figure 7. Influence of mycelial morphology and concentration on the number (a) and volume (b) of free air bubbles per frame.

concentration was higher. This behavior could be explained by the reduced number of big bubbles at the wall region (discussed above). At high biomass concentrations of dispersed mycelia, big bubbles were scarce in the image capture region, and therefore they are not expected to be immersed in oil drops.

Distribution of Free and Oil-Trapped Bubbles. Under the studied conditions, the oil showed a pronounced tendency to entrain both air bubbles and what we consider to be water droplets, leading to the formation of complex oil drops (Figure 2). The immersion of droplets and bubbles in oil drops could obviously affect substrate availability to the microorganism in the actual fermentation system, as the interfacial area of dispersed phases could be modified. On the other hand, bubble inclusion in oil drops might have important implications on oxygen transfer, as oxygen transfer from a bubble to a viscous oil is different from the conventionally assumed mechanism of oxygen transfer from a bubble to an aqueous medium (*21*). Due to a higher oxygen solubility in oil compared to that in aqueous medium, oxygen transfer rate is expected to increase with the relative volume of air bubbles inside oil drops.

Sajjadi et al. (*32*) stated that droplet inclusion in drops depends on the dispersed phase ability to incorporate the continuous phase and such ability is greatly improved by the presence of an appropriate surfactant in the dispersed phase. Two mechanisms of droplet inclusion have been described in detail by Sajjadi et al. (*32*). These authors mentioned that internal droplets may be formed when the continuous phase is trapped between coalescing drops. This entrainment is most probable when at least four drops collide, as the continuous phase—enclosed in the colliding drops—entrains as a newly formed drop (*33*). The second mechanism suggests that droplet inclusion could also occur by drop deformation, which may ease the continuous phase incorporation into the dispersed phase.

In the present study, after 2 h of stabilization, when the first set of images (for the control run) were captured, oil drops showed a high number of what we consider to be water droplets immersed. The presence of air in the system showed a strong effect on droplet immersion in drops. Considering the nonaerated and aerated systems without biomass, under nonaerated conditions, oil drops practically did not exhibit droplets inclusion, and most of the drops showed smooth surfaces. However, in the aerated case, the oil drops had an appearance suggesting a high number of internal droplets. The enhanced tendency of the dispersed phase to entrain droplets with aeration is postulated to be a result of larger oil drop sizes generated in the aerated system (d_{32} = 1222 μm) compared to the unaerated case (d_{32} = 644 μm), as a consequence of the drop in power drawn (Pg/P = 0.74) with aeration. An enhanced droplet immersion is ex-

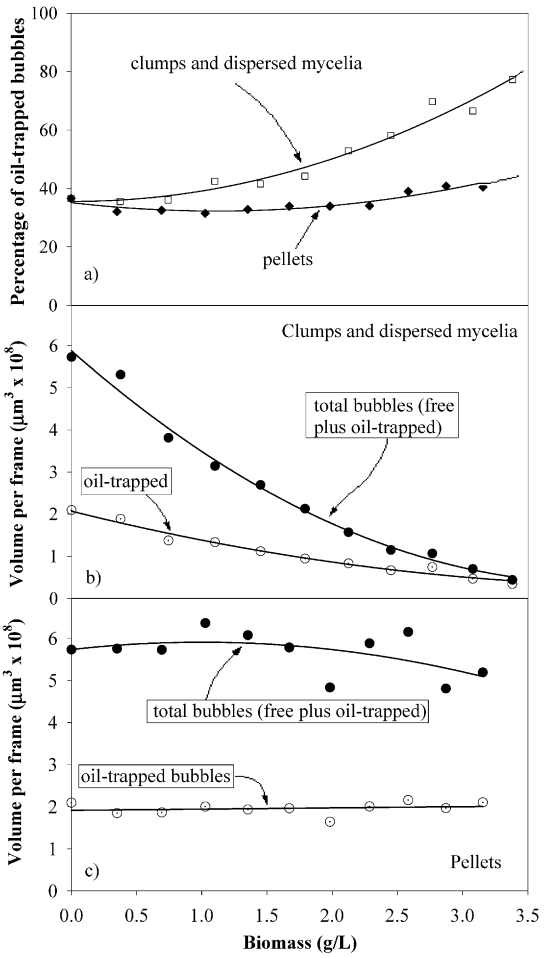

Figure 8. Percentage (in volume) of air bubbles in oil drops as a function of biomass morphology and concentration (a). Volume of oil-trapped and total bubbles per frame with dispersed mycelia (b) and pellets (c).

pected when larger oil drops are formed, since coalescence is favored and, as mentioned above, both entrainment and inclusion of droplets are likely to occur during the coalescing mechanism. Additionally, it is possible that when a free bubble is getting inside an oil drop, it could simultaneously be involved in the actual collision events responsible of entrainment and inclusion of droplets in drops, and an enhanced droplet inclusion is expected due to the presence of bubbles.

Measurements of droplets immersed in oil drops was not possible, even when sharply focused images of the dispersion were obtained. The highly filled drops and the small sizes (less than 5 μm) of immersed droplets complicated their measurement. Higher objective magnifications were not used because by doing so, many of the drops were out of the space field focused at such magnifications, this due to the larger sizes of drops compared with those of droplets. Evidently, further studies on the complex structure of oil drops are needed.

We also investigated the effect of mycelial morphology on the proportion (percentage in volume) of oil-trapped bubbles. These results are shown in Figure 8a. A higher percentage of oil-trapped bubbles was determined in the system with dispersed mycelia than with pellets. Also, an increase in the percentage of oil-trapped bubbles (from 32 to 80%) was observed as dispersed mycelia concentration increased. In the system with pellets, around 32% of bubbles were oil-trapped, and this percentage was practically the same over the whole range of biomass concentration analyzed.

The increase in the percentage (in volume) of oil-trapped bubbles observed with dispersed mycelia (Figure 8a) is assumed to be a result of the reduced number and volume of free bubbles, mentioned above. The reduced number and volume of free bubbles (Figure 7a,b, respectively) near the tank wall, particularly at high biomass concentrations, could cause a decrease in the total volume of air dispersed in that zone. We hence determined the average volume of total bubbles (i.e. free plus oil-trapped bubbles) per frame and plotted it against biomass concentration (Figure 8b). A sharp decrease in the total volume of bubbles with biomass concentration was evident. Also, a decrease in the volume of oil-trapped bubbles per frame is illustrated in Figure 8b; however, it was much less pronounced than for total bubbles. The ratio between the volume of oil-trapped bubbles divided by the total volume of bubbles (parameter plotted in Figure 8a) was higher when biomass concentration of dispersed mycelia increased. In the system with pellets, no significant changes in both the total volume of bubbles and the volume of oil-trapped bubbles with biomass concentration were observed (Figure 8c), and, consequently, no significant changes in the percentage of oil-trapped bubbles were recorded (Figure 8a). In the first instance, we state that, as a result of the increased percentage of oil-trapped bubbles with dispersed mycelia, an increase in oxygen transfer would be expected in the system with dispersed mycelia. At the other hand, the percentage of oil-trapped bubbles is practically constant with the pelleted morphology, and therefore the oxygen transfer is expected to be unaffected by biomass concentration. However, more studies are required in order to correlate oxygen transfer and the volume of oil-trapped bubbles.

Conclusions

By simulating the culture conditions of a four-phases fermentation involving *Trichoderma harzianum*, oil and air dispersion characteristics as a function of mycelial morphology was characterized. Sharp images of the dispersions were obtained, and the interaction of mycelial particles with bubbles and oil drops could be seen. Drop and bubble sizes changed depending upon the morphological type of biomass (pellets or dispersed mycelia) added to the system. At high biomass concentrations, larger oil drop sizes were observed in the presence of dispersed mycelia than with pellets. This behavior could be explained by the differences in the rheological properties of the suspensions. For the dispersed mycelia, higher biomass concentration resulted in higher broth viscosity, which caused a drop in power drawn and consequently, larger oil drop sizes were generated. Smaller bubble (free and oil-trapped) sizes were observed with dispersed mycelia, as compared with pellets. Also, a decrease in bubble sizes with higher dispersed mycelia concentration was observed. This lower size of bubbles was caused by the measurement of practically only small bubbles close to the tank wall (where the image capture point is located). Visual observation as well as a sharp decrease in the average number and volume of bubbles per frame suggested important segregation in the dispersed mycelia system, which can explain the unexpected small bubble sizes under such conditions. Bubble location was a function of the biomass type: the volume of oil-trapped bubbles increase (from 32 to 80%) with biomass concentration in the system with dispersed mycelia, while with pellets a practically constant (32%) percentage of oil-

trapped bubbles was determined. The observed interactions between the involved phases and the formation of complex oil drops should be considered in order to mechanistically explain mass transfer in these complex fermentations.

Acknowledgment

We thank the financial support of DGAPA-UNAM (Grant IN-105500) and CONACyT (S. Lucatero scholarship). We thank B. I. Taboada-Ramirez for technical assistance in image processing. We also thank J. A. Rocha-Valadez, M. S. Córdova, N. O. Pulido, and J. M. Baizabal for carefully reading the manuscript and helpful discussions.

Notation

d	baffle diameter, m
D	impeller diameter, m
d_{32}	Sauter diameter, μm
T	vessel diameter, m
K	consistency index, Pa s^n
n	flow index
P	power consumption under nonaerated conditions (W/m^3)
Pg	power consumption under aerated conditions (W/m^3)
vvm	vol of air/vol of liquid/minute (min^{-1})

References and Notes

(1) Bennett, J. W. Mycotechnology: The role of fungi in biotechnology. *J. Biotechnol.* **1998**, *66*, 101−107.
(2) Serrano-Carreón, L.; Flores, C.; Galindo, E. γ-Decalactone production by *Trichoderma harzianum* in a stirred bioreactor. *Biotechnol. Prog.* **1997**, *13*, 205−208.
(3) Bonnarme, P.; Djian, A.; Latrasse, A.; Féron, G.; Ginies, C.; Durand, A.; Le Queré, J. L. Production of 6-pentyl-α-pyrone by *Trichoderma* sp. from vegetable oils. *J. Biotechnol.* **1997**, *56*, 143−150.
(4) Li, C. Y.; Cheng, C. Y.; Chen, T. L. Production of *Acinetobacter radioresistans* lipase using Tween 80 as the carbon source. *Enzyme Microb. Technol.* **2001**, *29*, 258−263.
(5) Large, K. P.; Ison, A. P.; Williams, D. J. The effect of agitation rate on lipid utilization and clavulanic acid production in *Streptomyces clavuligerus*. *J. Biotechnol.* **1998**, *63*, 111−119.
(6) Calabrese, R. V.; Chang, T. P. K.; Dang, P. T. Drop break up in turbulent stirred-tank contactors. Part I: Effect of dispersed phase viscosity. *AIChE J.* **1986**, *32*, 657−666.
(7) Hinze, J. O. Fundamentals of the hydrodynamic mechanism of splitting dispersion process. *AIChE J.* **1955**, *1*, 289.
(8) Marten, M. R.; Velkovska, S.; Khan, S. A.; Ollis, D. F. Rheological, mass transfer, and mixing characterization of cellulase-producing *Trichoderma reesei* suspensions. *Biotechnol. Prog.* **1996**, *12*, 602−611.
(9) Zhao, S.; Kuttuva, S. G.; Ju, L. K. Oxygen transfer characteristics of multiple-phase dispersions simulating water-in-oil xanthan fermentations. *Bioprocess Eng.* **1999**, *20*, 313−323.
(10) Pazouki, M.; Panda, T. Understanding the morphology of fungi. *Bioprocess Eng.* **2000**, *22*, 127−143.
(11) Su, W. W.; He, B. J. Secreted enzyme production by fungal pellets in a perfusion bioreactor. *J. Biotechnol.* **1997**, *54*, 43−52.
(12) Braun, S.; Vecht-Lifshitz, S. E. Mycelial morphology and metabolite production. *Trends Biotechnol.* **1991**, *9*, 63−68.
(13) Olsvik, E.; Tucker, K. G.; Thomas, C. R.; Kristiansen, B. Correlation of *Aspergillius niger* broth rheological properties with biomass concentration and the shape of mycelial aggregates. *Biotechnol. Bioeng.* **1993**, *42*, 1046−1052.
(14) Olsvik, E.; Kristiansen, B. Rheology of filamentous fermentations. *Biotechnol. Adv.* **1994**, *12*, 1−39.
(15) Nienow, A. W.; Elson T. P. Aspects of mixing in rheologically complex fluids. *Chem. Eng. Res. Des.* **1988**, *66*, 5−15.
(16) Kawase, Y.; Araki, T.; Shimizu, K.; Miura, H. Gas−liquid mass transfer in three-phase stirred tank reactors: Newtonian and non-Newtonian fluids. *Can. J. Chem. Eng.* **1997**, *75*, 1159−1164.
(17) Shimizu, K.; Minekawa, K.; Hirose, T.; Kawase, Y. Drop breakage in stirred tanks with Newtonian and non-Newtonian fluid systems. *Chem. Eng. J.* **1999**, *72*, 117−124.
(18) Allen, D. G.; Robinson, C. W. The prediction of transport parameters in filamentous fermentation broths based on results obtained in pseudoplastic polymer solutions. *Can. J. Chem. Eng.* **1991**, *69*, 498−505.
(19) Boye, A. M.; Lo, M. Y. A.; Shamlou, P. A. The effect of two-liquid phase rheology on drop breakage in mechanically stirred vessels *Chem. Eng. Commun.* **1996**, *143*, 149−167.
(20) Galindo, E.; Pacek, A. W.; Nienow, A. W. A study of drop and bubble sizes in a simulated, mycelial fermentation broth of up to four phases. *Biotechnol. Bioeng.* **2000**, *69*, 213−221.
(21) Larralde, P.; Cordova, M. S.; Galindo, E. Distribution of the free and oil-trapped air bubbles in simulated broths containing fungal biomass. *Can. J. Chem. Eng.* **2002**, *80*, 491−494.
(22) Thomas, C. R. Image analysis: Putting filamentous microorganisms in the picture. *Trends Biotechnol.* **1992**, *10*, 343−348.
(23) Reséndiz, R.; Martínez, A.; Ascanio, G.; Galindo, E. A new pneumatic bearing dynamometer for power input measurement in stirred tanks. *Chem. Eng. Technol.* **1991**, *14*, 105−108.
(24) Taboada, B.; Larralde, P.; Brito, T.; Vega-Alvarado, L.; Díaz, R.; Galindo, E.; Corkidi, G. Images acquisition of multiphase dispersion in fermentation processes. *J. Appl. Sci. Technol.*, in press.
(25) Fatile, I. A. Rheological characteristics of suspensions of *Aspergillus niger*: Correlation of rheological parameters with microbial concentration and shape of the mycelial aggregate. *Appl. Microbiol. Biotechnol.* **1985**, *21*, 60−64.
(26) Riley, G. L.; Tucker, K. G.; Paul, G. C.; Thomas, C. R. Effect of biomass concentration and mycelial morphology on fermentation broth rheology. *Biotechnol. Bioeng.* **2000**, *68*, 160−172.
(27) Pelton, R.; Piette, R. Air bubble holdup in quiescent wood pulp suspensions. *Can. J. Chem. Eng.* **1992**, *70*, 660−663.
(28) Doyle, R,; Rosenberg, M. *Microbial cell surface hydrophobicity*; American Society for Microbiology: Washington, D.C., 1990.
(29) Pacek, A. W.; Man, C. C.; Nienow, A. W. Coalescence rates in water (aqueous)-in-oil and in oil-in-water (aqueous) dispersions (Paris, Récents Progrès en Génie des Procédés). *Proc. 9th Eur. Mixing Conf.* **1997**, *11* (52), 263−276.
(30) Moran, K.; Yeung, A.; Masliyah, J. Factors affecting the aeration of small bitumen droplets. *Can. J. Chem. Eng.* **2000**, *78*, 625−634.
(31) Rocha-Valadez, J. A.; Galindo, E.; Serrano-Carreón, L. Effect of the impeller-sparger configuration over *Trichoderma harzianum* growth in four-phases cultures under constant dissolved oxygen. *Bioprocess Eng.* **2000**, *23*, 403−410.
(32) Sajjadi, S.; Zerfa, M.; Brooks, B. W. Dynamic behaviour of drops in oil/water/oil dispersions. *Chem. Eng. Sci.* **2002**, *57*, 663−675.
(33) Brooks, B. W.; Richmond, H. N. Phase inversion in nonionic surfactant-oil-water systems-II. Drop size studies in catastrophic inversion with turbulent mixing. *Chem. Eng. Sci.* **1994**, *49*, 1065−1075.

Accepted November 18, 2002.

BP020118E